Computación y Sistemas Número Especial pp. 108 - 116
© 2002, CIC - IPN. *ISSN 1405-5546* Impreso en México

A Phase Domain Modelling of Thyristor Controller Series Compensator for Active Power Flow Control in Unbalanced Electric Transmission Networks

Modelado en el Dominio de Fases del Compesador Serie Controlado por Tristores para el Control de Flujo de Potencia Activa en Redes de Transmisión Eléctricas Desbalanceadas

Tiberio Venegas Trujillo, Claudio R. Fuerte Esquivel and **José L. Guardado Zavala**
Programa de Graduados en Eléctrica
Instituto Tecnológico de Morelia, Mich. México CP. 58120
E-mails: cfuerte@antares.tecmor.mx, cfuerte@hotmail.com

Article received on June 19, 2001; accepted on February 19, 2002

Resumen

En este artículo se desarrolla un modelo matemático estacionario del Compensador Serie Controlado por Tiristores (CSCT), el cual esta forma parte de los nuevos controladores electrónicos actualmente desarrollados dentro del concepto de Sistemas Flexible de Transmisión en Corriente Alterna (SIFLETCA). El modelado se efectúa en el dominio de fases considerando la estructura física del CSCT. Un programa para el análisis de flujos de potencia en redes desbalanceadas basado en el método de Newton es desarrollado para incluir el modelo propuesto y cuantificar su efecto en la red eléctrica. Las ecuaciones de flujo de potencia de la red eléctrica y el CSCT se resuelven de manera simultanea en un solo marco de referencia obteniéndose una solución iterativa robusta. El efecto del CSCT se cuantifica en redes eléctricas operando en estado balanceado y desbalanceado.
Palabras Clave: *SIFLETCA, CSCT, Control de Flujo de Potencia, Newton Raphson.*

Abstract

The goal of this paper is to develop a steady-state mathematical model of the new generation of power electronic-based plant components presently emerging as a result of the newly developed concept of Flexible AC Transmission Systems (FACTS), namely Thyristor Controlled Series Compensator (TCSC). The modelling is carried out in the phase domain considering the TCSC physical structure. A polyphase power flow program based on Newton Algorithm is developed in order to implement the proposed model. The power flow equations pertaining to TCSC controller and the electrical network are solved simultaneously in a unified frame-of-reference for highly robust iterative solutions. Analysis of the TCSC performance is carried out in both balanced and unbalanced power network operating conditions.
Keywords: *FACTS, TCSC, Power Flow Control, Newton Raphson.*

List of principal symbols

P, Q	Active and Reactive nodal power injections.
V, θ	Nodal voltage magnitude and angle.
G, B	Admittance real and imaginary parts.
$\Delta P, \Delta Q$	Active and reactive nodal power mismatch.
J	Jacobian matrix of partial derivatives of active and reactive powers with respect to nodal voltage magnitude and angles.
α	Thyristor firing angle.
R, X	Impedance real and imaginary parts.

1 Introduction

As electric utilities moves into a more competitive generation supply regimes with limited scope to expand their transmission facilities, the optimisation of existing transmission corridors for power transfer becomes of paramount importance. In this scenario, FACTS technologies appear as an attractive alternative to increase system operation flexibility (Hingorani 1993). The FACTS concept is based on the incorporation of power electronic devices into the high voltage side of the power network so as to make the network electronically controllable.

Some of high voltage and high current power electronics controllers have been in use from early 1970's such as High-Voltage DC transmission (HVDC) or Static VARs Compensators (SVC). Based on the experience gained on the applications of these power plant components, together with the fast development of semiconductor technologies, a wide range of controllers have been proposed to enhance network controllability and increase power transfer capability. In this context, the Thyristor Controller Series Capacitor (TCSC) has today reached maturity in its concept and applications.

Despite the series compensation has been in commercial use since early 1960s, the incorporation of a thyristor control has enable further flexibility so as active power flow control, power flow balancing and damping of power oscillations, among others. Figure 1 shows a schematic representation of a TCSC module [Christ et al., 1992], which is based on a thyristor-controlled reactor connected in parallel with a fixed capacitor. From a steady-state point of view, the TCSC allows a rapid and continuous change of the compensated transmission line apparent impedance. Hence, the TCSC is able to schedule directly power flow along desired paths and allows the system to operates close to the line limits.

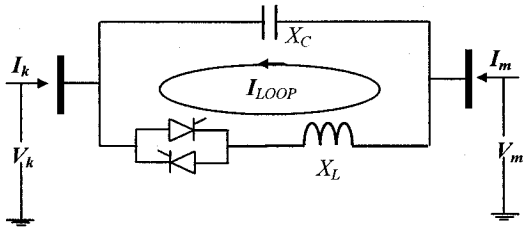

Figure. 1 TCSC module.

A co-operative effort between electric companies, universities and research institutes is being carried out in order to assist power systems engineers to assess the effects of TCSC devices on transmission system's performance. Before meaningful results can be obtained from application studies, realistic mathematical models for the transmission system and TCSC controllers need to be realised, coded and extensively verified. In this context, a power flow program should offer a very useful tool for system planners and operators to evaluate the technical and economic benefits of alternative solutions offered by the TCSC technology.

Opposite to the conventional power plant transmission components, the TCSC controller has a time-varying topology, which in turn interacts with the power system to produces imbalances. Hence, in order to achieve the nearest representation to the reality of a power system containing TCSC controllers, it is necessary to develop their modelling and analysis in the phase co-ordinates. Bearing this in mind, this paper focuses on the development of a steady-state TCSC power flow model in the phase frame of reference.

2 Power Flow Analysis of Networks with FACTS Devices

In its most basic form the power flow problem involves solving the set of non-linear algebraic equations which represent the electric network under steady state conditions. The reliable solution of real life transmission and distribution networks is not a trivial matter and Newton-type methods, with their strong convergence characteristics, have proved most successful (Tinney and Hart, 1967; Stott, 1974).

The nodal power flow equations,

$$P = f(V,\theta,G,B) \tag{1}$$

$$Q = g(V,\theta,G,B) \tag{2}$$

and their linearisation around a base point, (P^0,Q^0),

$$\begin{bmatrix}\Delta P\\ \Delta Q\end{bmatrix}^i = \begin{bmatrix}J\end{bmatrix}^i \begin{bmatrix}\Delta\theta\\ \Delta V\end{bmatrix}^i \tag{3}$$

are already well documented (Tinney and Hart, 1967).

Over the years, special algorithms have been put forward which have addressed the modelling of controllable devices in Newton's method, such as Load Tap Changing (LTC) and phase-shifting transformers, series and shunt variable compensation. A long list of published work in this area proposes algorithms based on a sequential solution. However, a major drawback in all these methods is that the nodal voltage magnitudes and angles are the only state variables which are calculated in true Newton fashion, whilst a sub-problem is formulated for updating the state variables of the controllable devices at the end of each Newton-Raphson iteration. This sequential iterative approach is rather attractive because it is straightforward to implement in existing Newton-Raphson programs but caution has to be exercised because it will yield no quadratic convergence.

A fundamentally different approach for the solution of controlled devices within the context of the power flow problem was developed at a very early stage by Peterson and Meyer [1971]. It is a highly efficient method which combines the state variables corresponding to the controllable devices with the nodal voltage magnitudes and angles of the network in a single frame-of-reference for a unified iterative solution. The method retains Newton's quadratic convergence characteristics. Two types of controllable devices were addressed, namely LTCs and phase-shifting transformers. This method is not necessarily easy to implement. It requires the Jacobian matrix to be modified in order to incorporate the contributions corresponding to LTCs and phase-shifters. In this iterative environment the state variables of a LTC are adjusted automatically so as to satisfy a specified voltage magnitude and the state variables of a phase shifter are adjusted automatically so as to satisfy a specified power flow.

We are aware of the limitations exhibited by non-compliant Newton-Raphson techniques and the early work of Peterson and Meyer has been extended in this paper to encompass a Thyristor Controlled Series Compensator.

3 Background and Motivation Behind the Present Work

A comprehensive theory covering the steady state modelling and analysis of power systems in phase co-ordinates was developed and reported by Laughton [1968] in the late 1960s. Wasley and Shlash [1974] reported the first three-phase power flow algorithm based on the Newton-Raphson (NR) method. In this article the generators are modelled as balanced injections of active and reactive powers. From this publication onwards, extensions and applications of phase co-ordinate power flow analysis to transmission systems have been published. In 1976, Birt, Graffy, McDonald and El-Abiad [1976] improved the representation of the synchronous machine by considering two generator buses, namely internal bus and generator terminals. The internal bus represents balanced induced voltages. On the other hand, the voltages at the generator terminals are function of the network operative conditions. The generator voltage regulator was also taken into account. Both models were included in a NR three-phase load flows program. In 1978, Arrillaga and Harker [1978]

developed a decoupled three-phase power flow algorithm, which was further extended (Harker and Arrillaga, 1979), by considering a 12 pulses HVDC link. The HVDC model was carried out in phase co-ordinates and allows representing different control options over the AC-DC converter variables. Xu, Marti and Dommel [1991] developed a three-phase algorithm based on branch current formulation rather than a nodal method. The proposed algorithm allows to take into account special connections in generators and loads, e.g. delta connections, with a great flexibility. However, a great disadvantage is that the Jacobian matrix presents null diagonal elements, which may not be "filled" during the Gaussian elimination process. Hence, the natural order of elimination of the offending diagonal element should be delaying, until a non-zero element is created in that location during the elimination process. Very recently, a new formulation has been reported which performs three-phase power flow calculations using the current injection method [Garcia et al., 2000]. Opposite to the conventional power flow formulation, the nodal mismatches are based on the current injected at every system's node. The Jacobian matrix has the same structure as the nodal admittance matrix. Furthermore, except to the *PV* nodes, the Jacobian elements are equal to those of the nodal admittance matrix.

Despite of the long list of work reported on power flow analysis in phase co-ordinates, only a few papers take into account controllable components (Harker and Arrillaga, 1979; Wortman et al., 1985; Xu et al., 1991). Additionally, in this context, very little work has been reported on power flow models taking into consideration thyristor based controllers (Harker and Arrillaga, 1979; Xu et al., 1991). Bearing this in mind, and based on a positive-sequence TCSC power flow model recently reported (Fuerte-Esquivel et al., 2000), this paper presents the progress on tackling the steady-state, phase co-ordinate modelling and analysis of TCSC devices. An existing Object Oriented Programming (OOP) polyphase power flow program (Fuerte-Esquivel et al, 1998) has been extended to encompass the TCSC model. A benchmark network has been used in order to show the prowess of the TCSC device to control of active power. Detailed numerical simulations are provided so as to enable potential users of this model to make any comparisons.

4 TCSC Fundamental Impedance

The TCSC fundamental impedance is obtained by solving the ordinary differential equations involving the TCSC voltages and currents. The solution of these equations provides analytical expressions, which are subjected to a Fourier transform analysis in order to derive current phasor expressions at the fundamental frequency. When the thyristor is turned-off, the capacitor current is identical to the line current and leads the capacitor voltage by 90°. The thyristor turn-on produces a voltage across the inductor equal in magnitude and phase to the capacitor voltage. This voltage drives a current through the inductor which lags 90° the voltage waveforms, and it is opposite in magnitude to the capacitor current, producing a loop current. This loop current has a distorting effect on the voltage waveform across the TCSC terminals.

An expression for the TCSC fundamental impedance that includes the loop current is (Fuerte-Esquivel et al, 2000),

$$X_{TCSC(1)} = -X_C + C_1\left(2(\pi-\alpha)+\sin(2(\pi-\alpha))\right) - C_2\cos^2(\pi-\alpha)\left(\varpi\tan(\varpi(\pi-\alpha)) - \tan(\pi-\alpha)\right) \quad (4)$$

where

$$X_{LC} = \frac{X_C X_L}{X_C - X_L} \quad , \quad \varpi = \sqrt{\frac{X_C}{X_L}} \quad (5)$$

$$C_1 = \frac{X_C + X_{LC}}{\pi} \quad , \quad C_2 = \frac{4X_{LC}^2}{X_L \pi} \quad (6)$$

5 TCSC Power Flow Model

A TCSC can be seen as an adjustable susceptance, $B_{TCSC(1)}$ (reactance $X_{TCSC(1)}$), as a function of the firing angle value. In this case, $B_{TCSC(1)}$ adjust itself to constraint the active power flow at a specified value, along the compensated transmission line.

In general, the transfer admittance matrix for the TCSC connected between nodes *k* and *m* is,

$$\begin{bmatrix} I_k^\rho \\ I_m^\rho \end{bmatrix} = \begin{bmatrix} jB_{kk}^\rho & jB_{km}^\rho \\ jB_{mk}^\rho & jB_{mm}^\rho \end{bmatrix} \begin{bmatrix} V_k^\rho \\ V_m^\rho \end{bmatrix} \quad (7)$$

where ρ indicates the phase analysed, i.e. *a, b, c*. Owing to the fact that the TCSC phases are decoupled, B^ρ_{ij} (i=*k,m* and j=*k,m*) is a diagonal matrix. In this case, the power flow formulation can be carry out by phase. The transfer admittance matrix elements are,

$$B_{kk}^\rho = B_{mm}^\rho = B_{TCSC(1)}^\rho = -\frac{1}{X_{TCSC(1)}^\rho}$$
$$B_{km}^\rho = B_{mk}^\rho = -B_{TCSC(1)}^\rho = \frac{1}{X_{TCSC(1)}^\rho} \quad (8)$$

The TCSC power equations at node *k* are [Fuerte-Esquivel et al., 2000],

$$P_k^\rho = -V_k^\rho V_m^\rho B_{TCSC(1)}^\rho \sin\left(\theta_k^\rho - \theta_m^\rho\right) \quad (9)$$

$$Q_k^\rho = -(V_k^\rho)^2 B_{TCSC(1)}^\rho + V_k^\rho V_m^\rho B_{TCSC(1)}^\rho \cos\left(\theta_k^\rho - \theta_m^\rho\right) \quad (10)$$

The TCSC linearised power equations with respect to the firing angle are,

$$\frac{\partial B_{TCSC(1)}^\rho}{\partial \alpha^\rho} = (B_{TCSC(1)}^\rho)^2 \frac{\partial X_{TCSC(1)}^\rho}{\partial \alpha^\rho} \quad (11)$$

$$\frac{\partial P_k^\rho}{\partial \alpha^\rho} = P_k^\rho B_{TCSC(1)} \frac{\partial X_{TCSC(1)}^\rho}{\partial \alpha^\rho} \quad (12)$$

$$\frac{\partial Q_k^\rho}{\partial \alpha^\rho} = Q_k^\rho B_{TCSC(1)} \frac{\partial X_{TCSC(1)}^\rho}{\partial \alpha^\rho} \tag{13}$$

where

$$\begin{aligned}\frac{\partial X_{TCSC(1)}^\rho}{\partial \alpha^\rho} &= -2C_1^\rho\left(1+\cos(2\alpha^\rho)\right) \\ &+ C_2^\rho sin(2\alpha^\rho)\left(\omega\, tan(\omega(\pi-\alpha^\rho)) - tan\alpha^\rho\right) \\ &+ C_2^\rho\left(\omega^2 \frac{\cos^2(\pi-\alpha^\rho)}{\cos^2(\omega(\pi-\alpha^\rho))} - 1\right)\end{aligned} \tag{14}$$

When the TCSC module is controlling the active power flowing from nodes k to m, at a specified value, the set of linearised power flow equations is given by (15). $\Delta P_{km}^{\rho,\alpha} = P_{km}^{\rho,\alpha,\mathrm{Reg}} - P_{km}^{\rho,\alpha,cal}$ is the active power flow mismatch for TCSC module and $\Delta\alpha^\rho = \alpha^{\rho,j+1} + \alpha^{\rho,j}$ is the incremental change in the TCSC's firing angle. $P_{km}^{\rho,\alpha,cal} = P_k^\rho$ and the superscript i indicates iteration. For the equation at node m exchange the subscript k and m in (9) to (15).

$$\begin{bmatrix} \Delta P_k^\rho \\ \Delta P_m^\rho \\ \Delta Q_k^\rho \\ \Delta Q_m^\rho \\ \Delta P_{km}^{\rho,\alpha} \end{bmatrix}^i = \begin{bmatrix} \frac{\partial P_k^\rho}{\partial \theta_k^\rho} & \frac{\partial P_k^\rho}{\partial \theta_m^\rho} & \frac{\partial P_k^\rho}{\partial V_k^\rho}V_k^\rho & \frac{\partial P_k^\rho}{\partial V_m^\rho}V_m^\rho & \frac{\partial P_k^\rho}{\partial \alpha^\rho} \\ \frac{\partial P_m^\rho}{\partial \theta_k^\rho} & \frac{\partial P_m^\rho}{\partial \theta_m^\rho} & \frac{\partial P_m^\rho}{\partial V_k^\rho}V_k^\rho & \frac{\partial P_m^\rho}{\partial V_m^\rho}V_m^\rho & \frac{\partial P_m^\rho}{\partial \alpha^\rho} \\ \frac{\partial Q_k^\rho}{\partial \theta_k^\rho} & \frac{\partial Q_k^\rho}{\partial \theta_m^\rho} & \frac{\partial Q_k^\rho}{\partial V_k^\rho}V_k^\rho & \frac{\partial Q_k^\rho}{\partial V_m^\rho}V_m^\rho & \frac{\partial Q_k^\rho}{\partial \alpha^\rho} \\ \frac{\partial Q_m^\rho}{\partial \theta_k^\rho} & \frac{\partial Q_m^\rho}{\partial \theta_m^\rho} & \frac{\partial Q_m^\rho}{\partial V_k^\rho}V_k^\rho & \frac{\partial Q_m^\rho}{\partial V_m^\rho}V_m^\rho & \frac{\partial Q_m^\rho}{\partial \alpha^\rho} \\ \frac{\partial P_{km}^{\rho,\alpha}}{\partial \theta_k^\rho} & \frac{\partial P_{km}^{\rho,\alpha}}{\partial \theta_m^\rho} & \frac{\partial P_{km}^{\rho,\alpha}}{\partial V_k^\rho}V_k^\rho & \frac{\partial P_{km}^{\rho,\alpha}}{\partial V_m^\rho}V_m^\rho & \frac{\partial P_{km}^{\rho,\alpha}}{\partial \alpha^\rho} \end{bmatrix}^i \begin{bmatrix} \Delta\theta_k^\rho \\ \Delta\theta_m^\rho \\ \frac{\Delta V_k^\rho}{V_k^\rho} \\ \frac{\Delta V_m^\rho}{V_m^\rho} \\ \Delta\alpha^\rho \end{bmatrix}^i \tag{15}$$

6 Numerical Properties of the Model

The numerical behaviour of the TCSC mathematical model depends on the number of TCSC internal resonant points present in the range of 90° to 180°.

6.1 Numerical Properties with One Resonant Point

Figures 2 and 3 show the TCSC fundamental reactance and susceptance profiles, as function of the firing angle, respectively. The partial derivatives of these parameters with respect to the firing angle are also shown. The inductance and capacitance TCSC reactances were assumed to be 2.6 Ω and 15 Ω, respectively, at a base frequency of 60 Hz.

A resonant point takes place in the TCSC fundamental reactance at α_R = 142.81° as shown in Figure 2. This pole defines the transition from the inductive to the capacitive TCSC operative region as the firing angle value increases.

It should be noted that both $X_{TCSC(1)}$ and $\partial X_{TCSC(1)}/\partial\alpha$ present large variations in magnitude to small variations in firing angle near the resonant point, such that TCSC power equations and Jacobian terms become ill-conditioned in this region. On the other hand, it is clear from Figure 3 that $B_{TCSC(1)}$ and $\partial B_{TCSC(1)}/\partial\alpha$ profiles do not present discontinuities. Both vary in a continuous, smooth fashion in both operative regions. Hence, the power flow and Jacobian equations based on $B_{TCSC(1)}$ will exhibit better numerical behaviour than those based on $X_{TCSC(1)}$.

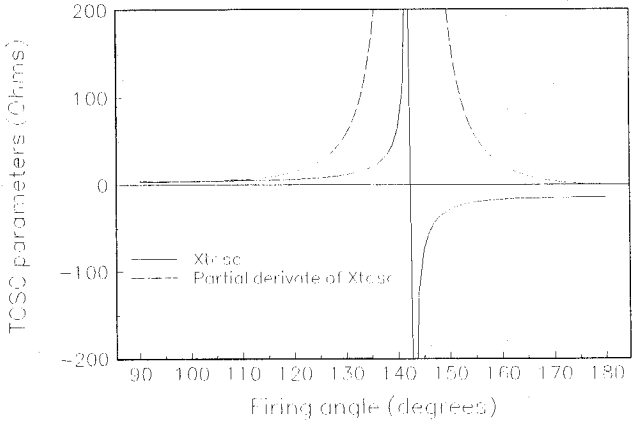

Figure 2. $X_{TCSC(1)}$ and $\partial X_{TCSC(1)}/\partial\alpha$ profile as function of firing angle

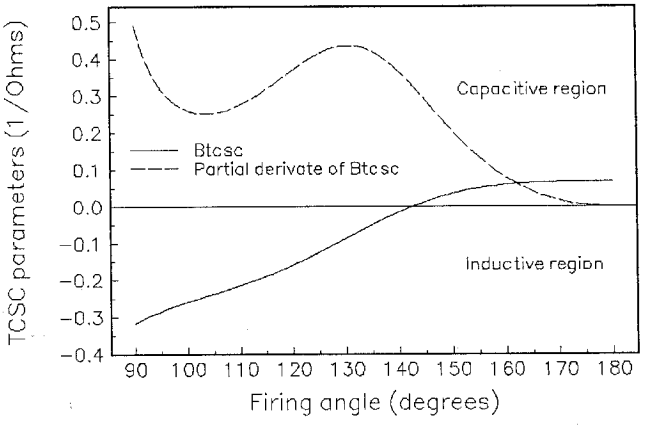

Figure 3. $B_{TCSC(1)}$ and $\partial B_{TCSC(1)}/\partial\alpha$ profile as function of firing angle

6.2 Numerical Properties with Multiple Resonant Points

By suitable modifying the TCSC inductive reactance values used in Section 6.1, it is possible to have a TCSC, which exhibits multiple resonant points. A values of X_C= 15 Ω and X_L = 1.0 Ω were chosen. The resulting profiles of $X_{TCSC(1)}$, $\partial X_{TCSC(1)}/\partial\alpha$ and $B_{TCSC(1)}$, $\partial B_{TCSC(1)}/\partial\alpha$ as function of the firing angle are shown in Figures 4 and 5, respectively.

The TCSC fundamental reactance changes from inductive to capacitive region at the resonant points taking place at $\alpha_{R1} = 110.29°$ and $\alpha_{R2} = 156.76°$, as shown in Figure 4. Moreover, there is a change from capacitive to inductive region at the zero located at $\alpha_Z = 143.324°$. Due to the zero in the $X_{TCSC(1)}$ profile, the TCSC fundamental susceptance $B_{TCSC(1)}$ profile has a pole, as shown in Figure 5. This, of course, affects adversely the good numerical properties of the power flow NR method, i.e. the good properties of the Jacobian equations based on $B_{TCSC(1)}$ are lost.

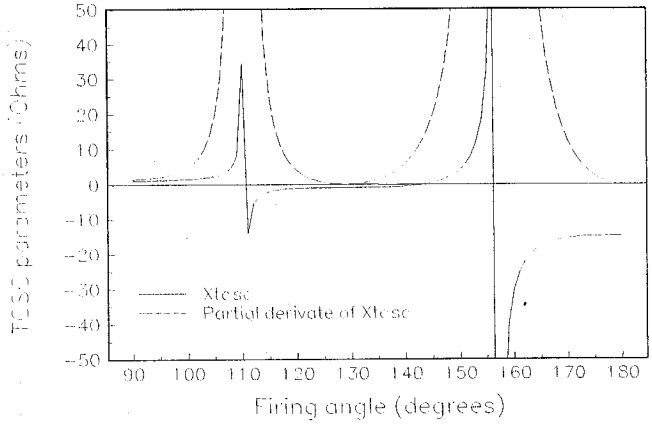

Figure 4. $X_{TCSC(1)}$ and $\partial X_{TCSC(1)}/\partial\alpha$ profile as function of firing angle

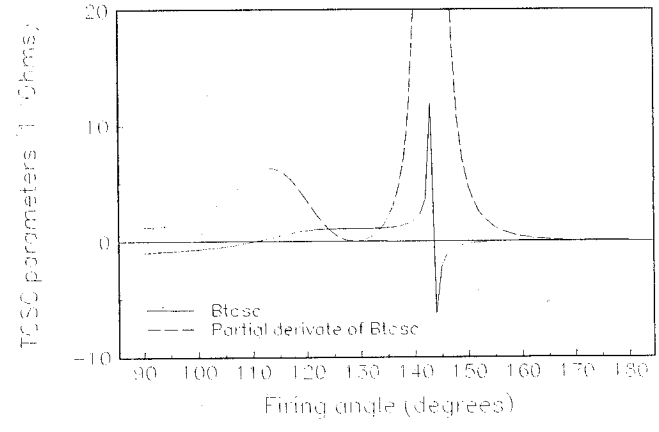

Figure 5. $B_{TCSC(1)}$ and $\partial B_{TCSC(1)}/\partial\alpha$ profile as function of firing angle

The analysis presented in Sections 6.1 and 6.2 concludes that TCSC capacitive and inductive reactance values should be chosen carefully in order to ensure that just one resonant point is present in the range 90° to 180°.

7 TCSC's Firing Angle Initial Condition

'Ill-chosen' starting conditions are often responsible for the Newton-Rapshon load flow solution diverging or arriving at some anomalous value. The hybrid method described in [Fuerte-Esquivel et al, 2000] is used in order to avoid an ill-conditioned Jacobian matrix if the customary zero voltage angle initialisation is used. The TCSC's firing angle is fixed, at the initial condition, until a pre-specified voltage angle difference at the controller's terminals takes place. The initial condition for the TCSC's firing angle is selected within the range of ±8° from the resonant point.

8 Truncated Adjustments

Even in cases when only one resonant point exist in the TCSC fundamental susceptance profile, large mismatch values in ΔP, ΔQ *and* ΔP_{km}, can take place in the early stages of the iterative process, resulting in poor convergence. The problem will be aggravated if the final level of compensation is near to the resonant point. In this case, large increments in the TCSC firing angle produce changes from the capacitive to the inductive operative regions, and vice versa, causing the solution to oscillate. These unwanted numerical problems are reduced by truncate the computed adjustments if they exceed a specified limit. Size of correction of the firing angle adjustment has been limited during the backward substitution to 5°. The truncated adjustment effect is propagated throughout the remaining of the backward substitution. The AC network state variables are truncated as explained in (Fuerte-Esquivel et al, 2000).

9 Test Cases

A TCSC Class has been written in order to incorporate the model and methods mentioned above into our OOP Polyphase Load Flow program. The program has been coded in C^{++}, and is suitable to run under UNIX or Windows environment. The driving force which has motivated the use of OOP is that one of the most difficult problems with power systems software, which is normally written in FORTRAN and following a top-bottom design, is its inflexible code which is costly to maintain and to adapt to the very specific needs and changing requirements of each utility. Details of program implementations are given in (Fuerte-Esquivel et al, 1998). The program has been applied to the solution of power networks of different sizes and operative conditions. For purpose of this paper, a benchmark network has been considered in order to show the prowess of the proposed model.

9.1 Control of Active Power Flow

A small 5-node network (Stagg and El-Abiad, 1968) has been transformed to a three-phase system in order to show the control capabilities of the TCSC model. The transmission system is considered symmetric with balanced loading. A TCSC is embedded in the transmission line connected between nodes South and Lake to increase active power flowing from South to Lake in 18% at each phase. Converge was obtained in 6 iterations. The final values of TCSC's total reactance required to achieve the specified active power flow control are shown in Table 1. Solutions details of the upgraded network are provided in the single-

line diagram shown in Figure 6. The behaviour of the maximum absolute power mismatches, as function of the number of iterations, is plotted in Figure 7. Since no TCSC limits violations took place, the algorithm converged quadratically to a very tight power mismatch tolerance of 10^{-12}.

Table 1. TCSC final firing angle and total reactance values

Compensated transmission line	Firing angle Model		Phase
	α (degrees)	$X_{TCSC(I)}$ (p.u.)	
South to Lake	148.324	-0.061096	A
	148.324	-0.061096	B
	148.324	-0.061096	C

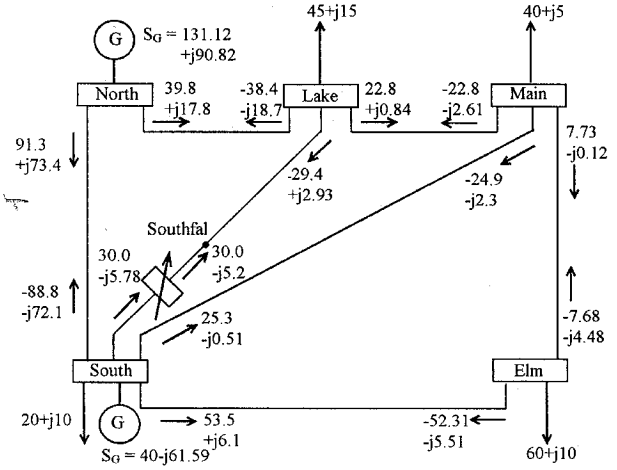

Figure 6. Modified balanced test network and load flow results

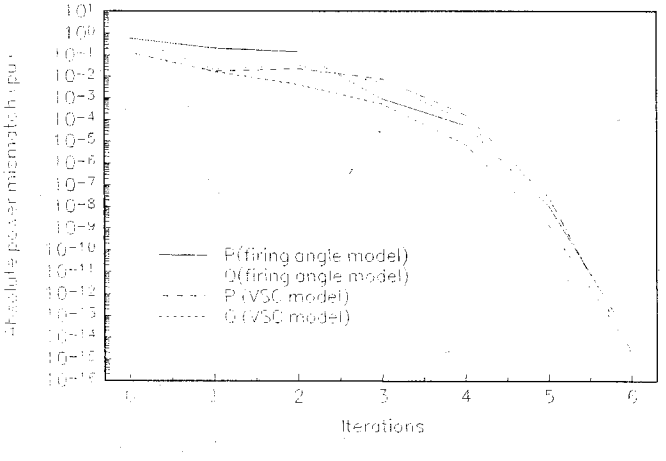

Figure 7. Power mismatches as function of number of iterations

9.2 TCSC Performance under Unbalanced Operating Conditions

Owing to the fact that the power flow control can be performed individually per phase, the TCSC allows to balance active power flow along the compensated transmission line under unbalanced operating conditions. The 5-node network used in last section is considered for this purpose. The load embedded at node Lake is assumed to have an unbalance of 20%. The active power flows in the transmission line connected between nodes South-Lake are shown in Table 2.

Table 2. Power flow from South to Lake due unbalanced loads

Loads at node Lake		Active power flow from South to Lake (MWs)	Phase
P(MWs)	Q(MVAr)		
54.00	18.00	27.3405	A
45.00	15.00	24.3646	B
36.00	12.00	21.7466	C

In order to circumvent the power flow asymmetries along South to Lake, this line is compensated with a TCSC, as shown in Fig. 6. The controller is intended to balance and maintain the active power flow at 35 MWs in each phase. The final results are shown in Table 3. The number of iterations required to converge was 7, and the TCSCs achieved the target control (Control Status 1). The analysis was carried out considering truncated adjustments. The level of compensation is computed based on the positive-sequence transmission line reactance.

Table 3. Final parameters of series compensators

Phase	α_{final} (degrees)	X_{final} (p.u.)	Control Status	% of Compensation.
A	144.415	-0.060786	1	(-) 33.77
B	143.403	-0.127887	1	(-) 71.04
C	143.420	-0.125532	1	(-) 69.74

9.3 Feasible Region of Control

Owing to the fact that the TCSC phases are electrically near they interact with each other. Hence, the amount of active power controlled by the device will be confined to a region in which the TCSC controller is within limits and the solution of the power flow equations exists. The feasible region is limited by the possible combination of the series controller minimum and maximum values. Figure 8 shows the feasible active power flow control region when the transmission line connected between South and Lake is compensated within the capacitive region by a TCSC. The maximum level of compensation in each phase was considered at 40% of the positive-sequence transmission line series inductive reactance value. The following combinations of series compensation give the boundary limits of the region.

1. Point A, VSC(a)= 1%, VSC(b)= 1% and VSC(c)= 1%
2. Point B, VSC(a)=40%, VSC(b)= 1% and VSC(c)= 1%
3. Point C, VSC(a)=40%, VSC(b)=40% and VSC(c)= 1%
4. Point D, VSC(a)=40%, VSC(b)=40% and VSC(c)=40%
5. Point E, VSC(a)= 1%, VSC(b)=40% and VSC(c)=40%
6. Point F, VSC(a)= 1%, VSC(b)= 1% and VSC(c)=40%
7. Point G, VSC(a)= 1%, VSC(b)=40% and VSC(c)= 1%
8. Point H, VSC(a)=40%, VSC(b)= 1% and VSC(c)=40%

Six cases were simulated in order to confirm the feasibility of the solution with both full and truncated adjustments. Table 4 shows the results in terms of required series compensation values to achieve the specified active power control. Control status 1 indicates that the TCSC upheld the specified target with compensation within limits.

From the results presented below, it can be observed that the TCSC upheld the target when the active power control was specified within limits of the feasible region. On the other hand, the TCSC hit its limits when the target is outside the feasible active power control region. In this case, the TCSC state variable is fixed at the offending limit (Control Status 0), and no further attempts are made at regulating the active power through the phase for the remaining of the iterative process.

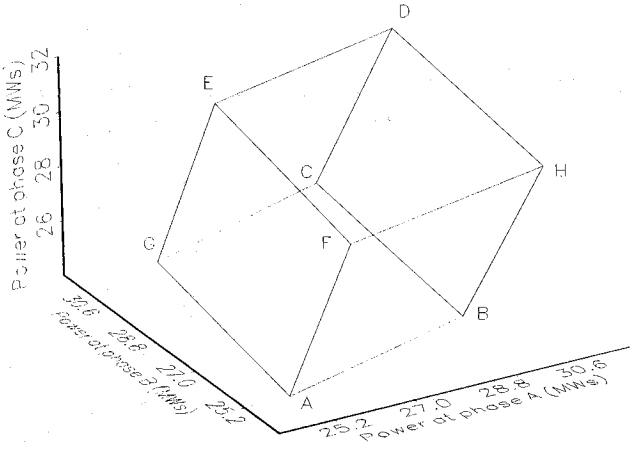

Figure 8. Feasible active power flow control region

Table 4. Final parameters of the TCSC

Case	Phase	Power (MWs)	X_{final} p.u.	Control Status	% of Compen.	Iterations Full	Iterations Trun
1	A	25	-0.006808	1	(-) 3.78	6	6
	B	25	-0.006808	1	(-) 3.78		
	C	25	-0.006808	1	(-) 3.78		
2	A	30	-0.061096	1	(-) 33.94	6	6
	B	30	-0.061096	1	(-) 33.94		
	C	30	-0.061096	1	(-) 33.94		
3	A	25	-0.001800	0	(-) 1.00	8	8
	B	27	-0.038612	1	(-) 21.45		
	C	30	-0.068223	1	(-) 37.90		
4	A	20	-0.001800	0	(-) 1.00	8	8
	B	20	-0.001800	0	(-) 1.00		
	C	20	-0.001800	0	(-) 1.00		
5	A	20	-0.001800	0	(-) 1.00	11	10
	B	25	-0.007641	1	(-) 4.24		
	C	35	-0.07200	0	(-) 40.00		
6	A	35	-0.07200	0	(-) 40.00	9	8
	B	35	-0.07200	0	(-) 40.00		
	C	35	-0.07200	0	(-) 40.00		

9.4 Multiple Resonant Points

In case of multiple resonant points, different TCSC's firing angle values can give the level of compensation required to achieve the specific active power flow. The TCSC parameters of the network analysed in Section 8.1 have been modified to those given in Section 5.2. Two different initial conditions α_0^p are specified. The simulated cases were carried out with truncated adjustments. The final results are shown in Table 5, where it is clear that multiple solutions take place depending of the initial condition selected.

Table 5. TCSC firing angle and reactances values

Case	TCSC South-Lake α_0^p (degrees)	α_{final}^p (degrees)	$X_{TCSC(1)}^p$ (p.u.)	Phase
1	115°	110.389°	-0.061096	A
	115°	110.389°	-0.061096	B
	115°	110.389°	-0.061096	C
2	165°	157.548°	-0.061096	A
	165°	157.548°	-0.061096	B
	165°	157.548°	-0.061096	C

The numeric examples described above were simulated with full adjustments in order to illustrate the potential problems of "ill-conditioned" iterative process when the solution takes place near to the resonant point. A comparative analysis on convergence performance is shown in Table 6. NC means non-convergence. These results clearly show the benefits of truncating the state variables correction step during the backward substitution. For the case of non-convergence, it was observed that the firing angle value was oscillating between the capacitive and inductive regions near to the resonant point.

Table 6. Number of iterations for the two kinds of adjustments

Type of adjustment	Iterations required to achieve convergence Case 1	Case 2
Full	NC	7
Truncated	6	8

10 Conclusions

A general phase co-ordinate TCSC power flow model has been presented in this paper. The TCSC's firing angle is taken as state variable, which is regulated in order obtain the level of compensation required to achieve the specified active power flow. This model has been included in a Newton-Raphson load flow algorithm, which is capable of solving power networks very reliably. The algorithm retains Newton's quadratic convergence and its efficiency has been illustrated by numeric examples. The influence of the TCSC firing angle size of correction, on convergence performance, has also been illustrated by numeric

examples. It has been shown that TCSC operation near resonance points degrades Newton's quadratic convergence. However, the algorithm has still shown to be very robust towards the convergence.

Acknowledgements

The authors gratefully acknowledge the financial assistance given by the Consejo Nacional de Ciencia y Tecnología (CONACyT), México under contract J28613-A

References

Arrillaga J. And **Harker B.J.**, "Fast Decoupled Three-Phase Load Flow", *Proceedings of IEE*, Vol. 125, No. 8, 1978, pp. 734-740.

Birt K.A., Graffy J.J. and **McDonald J.D.**, "Three Phase Load Flow Program", *IEEE Transactions on Power Apparatus and Systems*, Vol. PAS-95, No. 1, 1976, pp. 59-65.

Christl N., Hedin R., Sadek K., Lützelberger P., Krause P,E., McKenna S.M., Montoya A.H., and **Togerson D.**, "Advanced Series Compensation (ASC) with Thyristor Controlled Impedance", *CIGRÉ*, paper 14/37/38-05, Paris, September 1992.

Fuerte-Esquivel, C.R., Acha, E., Tan S.G and **Rico J.J.**, "Efficient Object Oriented Power systems Software for the Analysis of Large-Scale Networks containing FACTS-Controlled Branches", *IEEE Transactions on Power Systems*, Vol. 13, No. 2, 1998, pp.464-4722 .

Fuerte-Esquivel, C.R., Acha, E., and **Ambriz.Pérez, H.**, "A Thyristor Controlled Series Compensator Model for the Power Flow Solution of Practical Power Networks", *IEEE Transactions on Power System*, Vol. 15, No. 1, 2000, pp. 58-64.

Garcia P.A.N., Pereira J.L.R, Carneiro S., Da Costa V.M. and **Martins N.**, "Three-Phase Power Flow Calculations using the Current Injection Method", IEEE *Transactions on Power Systems,* Vol. 14, No. 4, 1999, pp. 1320-1326.

Harker B.J. and **Arrillaga J.** "3-Phase a.c./d.c. Load Flow", *Proceedings of IEE*, Vol. 126, No. 12, 1979, pp. 1275-1281.

Hingorani N.H., "Flexible AC Transmission Systems", *IEEE Spectrum*, April 1993, pp. 40-45.

Laughton M.A., "Analysis of Unbalanced Polyphase Networks by the Method of Phase Co-ordinates", *Proceedings of IEE*, Vol. 115, No. 8, 1968, pp. 1163-1172.

Peterson N.M. and **Scott Meyer W.,** "Automatic Adjustment of Transformer and Phase Shifter Taps in the Newton Power Flow", IEEE *Transactions on Power Apparatus and Systems*, Vol. PAS-90, No. 1, 1971, pp. 103-108.

Stagg G. W. and **El-Abiad A.,** *Computer Methods in Power System Analysis*, McGraw-Hill, New York, First Edition, 1968.

Stott B., "Review of Load-Flow Calculation Methods", IEEE *Proceedings*, Vol. 62, July 1974, pp. 916-929.

Tinney W.F. and **Hart C.E.,** "Power Flow Solution by Newton's Method", *IEEE Transactions on Power Apparatus and Systems*, Vol. PAS-96, No. 11, 1967, pp. 1449-1460.

Wasley R.G. and **Shlash M.A.,** " Newton-Rapshon Algorithm for 3-phase load flow", *Proceedings of IEE*, Vol. 121, No. 7, 1974, pp. 630-638.

Wortman M.A., Allen D.L. and **Grigsby L.L.,** "Techniques for the Steady State Representation of Unbalanced Power Systems: Part I. A Systematic Building Block Approach to Network Modeling", *IEEE Transactions On Power Apparatus and Systems*, Vol. PAS-104, No. 10, 1985, pp. 2805-2814.

Xu W., Marti J.R. and **Dommel H.W.,** "A Multiphase Harmonic Load Flow Solution Technique", *IEEE Transactions on Power Systems*, Vol. 6, No. 2, 1991, pp.174-182 .

Tiberio Venegas Trujillo, *received his BEng degree (Hons) from Universidad de Colima, México in 1996 and his MSc from the Instituto Tecnológico de Morelia , México in 2000. He is at present an Assistant Professor at the Universidad de Colima. His main research interests lie on the dynamic and steady-state analysis of FACTS.*

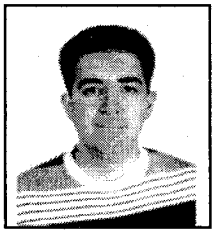

Claudio Rubén Fuerte Esquivel, *received his BEng degree (Hons) from Instituto Tecnológico de Morelia, México, in 1990, his MSc degree (Summa Cum Laude) from Instituto Politécnico Nacional, México, in 1993, and his PhD degree from the University of Glasgow, Scotland, UK in 1997. He is at present an Associated Professor at the Instituto Tecnológico de Morelia. His main research interests lie on the dynamic and steady-state analysis of FACTS, CUSTOM POWER and Real-Time Modelling and Analysis.*

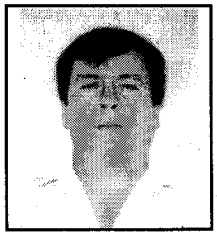

Jose Leonardo Guardado Zavala, *received his BSc degree in electrical engineering from UMSNH (Universidad Michoacana) in 1983. He also received the MSc (1986) and PhD (1989) degrees in electrical engineering from UMIST, Manchester UK. He joined IEE (Instituto de Investigaciones Eléctricas) in 1983 working in the modelling of switching transients in transmission lines and electrical equipment. He is actually a lecturer at the Instituto Tecnológico de Morelia in Michoacan, México.*